A NOVEL METHOD TO PROBE THE ORIGIN OF RADIO EMISSION IN LUMINOUS QUASARS

1 Scientific Justification

Executive Summary: In 2018B we initiated a pilot program to perform a novel test of the origin of radio emission in ostensibly radio-quiet luminous quasars. We adopted a typical flux density limit for the star-formation contribution and detected 22 of 50 objects using the S-band in the C-configuration. In 2021A we propose to extend our program to lower levels of star formation for the undetected targets, again using the S-band in the C-configuration. We will target 13 objects in sparse fields (i.e., without nearby bright sources to complicate the imaging) down to 3.65μJy, requiring roughly 3 hours per target.
Motivation: It is thought that there are at least four possible origins of radio emission in radio-quiet quasars (Kimball 2020, Panessa et al. 2019). In addition to the emission from (frustrated) jets there can be radio emission from star formation, the corona, and shocks from winds. Most investigations into the origin of radio emission from radio-quiet quasars focus either on low-redshift (Kimball et al. 2011b; Condon et al. 2013) or type-2 quasars (Zakamska & Greene 2014; Jarvis et al. 2019). Our program is unique in that it focuses on luminous quasars that are much more likely to host accretion disk winds than low-redshift samples and enables more universal indication of the accretion disk winds than high-redshift type-2 quasars.

In our pilot project we sought determine the fraction of quasars with radio emission in excess of that expected from star formation. The answer to that question will help to optimize the parameters of a broader investigation into differences in the origin(s) of radio emission from quasars. The ultimate *empirical* goal being understanding how emission-line parameters (as diagnostics of accretion disk winds) connect to the radio loudness. In turn we will achieve our *physics* goal of better understanding of what processes do (or do not) regulate the existence of radio emission in quasars from the central engine.

For example, if we find that quasars with strong winds *do* have intermediate radio emission between SF and strong jets, then it will be important to expand that sample. In that case, we will look to survey data from ongoing VLASS observations to determine which objects need new observations. Indeed archival VLA data already eliminated the need for new observations for 2 of our targets original 50 targets. However, this investigation cannot be conducted completely with survey data (e.g., FIRST, NVSS, or VLASS) as the flux density limits of all of those surveys are *far* too shallow. Nor can it be conducted with small-area deep pointings (e.g., COSMOS; Schinnerer et al. 2004) simply because a representative sample such as defined herein requires much larger sky areas.
Exploring Different Radio Origins: We now have the ability to recognize quasars whose spectra appear quite similar, but that have very different physical properties (e.g., as characterized by the Eddington ratio, $L/L_{\rm Edd}$; see Sulentic et al. 2007). These differences are correlated with the observed radio properties of quasars. For example, Richards et al. (2011) used a broad-emission-line diagnostic (derived from measurements of C IV) to show that neither are radio-loud sources uniformly distributed across this parameter space, nor do they occupy a distinct part of quasar parameter space apart from radio-quiet (RQ) quasars. Given the possibility of other origins for radio emission, it is important to distinguish additionally between jetted and non-jetted quasars (Padovani 2017) among those in the RL class. However, it is equally important to understand that RQ are not a monolithic class of objects either. Even within the relatively small dynamic range of the SDSS quasar catalog (as compared to the AGN population as a whole) there is quite a diversity of RQs and the radio properties are not uniform across that diversity (Richards et al. 2011; Kratzer & Richards 2015).

It is also important to further recognize that, in any parameter space one chooses, RQ quasars dominate over RL. Indeed the differences between the optical spectral properties of RL and RQ quasars are subtle at best (Kimball et al. 2011a; Schulze et al. 2017), spanning

nowhere near the full range of spectral properties that characterize quasar spectra (Boroson 2002; Richards et al. 2011). For the 0.4% of SDSS quasars that show radio lobes (Ivezic et al. 2002), it is pretty clear that the origin of the radio emission is synchrotron emission from jets (Urry & Padovani 1995). Probing to fainter (generally unresolved) radio flux densities, the radio emission is expected to be dominated by star formation processes that are unrelated to the central engine, either in the form of radio from free-free emission in HII regions produced by star formation or from synchrotron produced by relativistic electrons accelerated by SNe (Kimball et al. 2011b; Condon et al. 2013). Both AGN and SF sources of radio emission might be expected to depend on environment (e.g. Hickox et al. 2009; Retana-Montenegro & Rottgering 2017). Beyond star formation, it is also important to determine if some quasars really are radio silent, if there is evidence for weak frustrated jets (e.g., Barvainis et al. 1996; Blundell & Beasley 1998), coronal emission (Laor & Behar 2008; Raginski & Laor 2016; Laor et al. 2019), or shocks from winds interacting with gas in the host galaxy (Blundell & Kuncic 2007; Ciotti et al. 2010; Zakamska & Greene 2014). Our approach particularly addresses the question of potential radio emission due to winds, especially radiation-line-driven winds (e.g., Rankine et al. 2020). Herein we test the different possible origins of radio emission in luminous, high-redshift quasars from jets to shocks to star formation by observing a representative pilot sample of quasars down to the expected star-formation flux density limit (at the redshift of the quasars).

The Experiment: We use emission-line parameters from C IV (see Fig. 1) as a unique diagnostic of accretion disk winds. In 2018B we selected a random sample of 50 SDSS quasars at $z \sim 1.65$ (Schneider et al. 2007) in order to probe the full range of wind strengths. Our pilot program sought to target these quasars to 5x deeper than the "knee" of the radio luminosity function as determined by Magliocchetti et al. (2016). Our depth of 7.5uJy was sensitive to star-formation rates of 300-500 solar masses per year (for 3- and 5-σ detections, respectively).

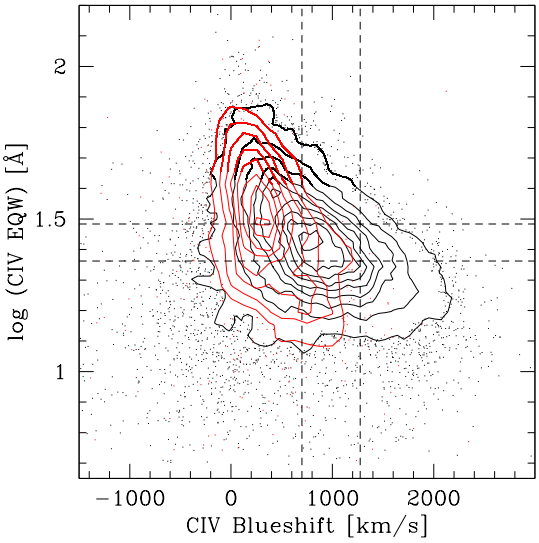

Figure 1: Distribution of SDSS quasars in C IV EQW vs. C IV blueshift space, which serves as the best empirical illustration of the diversity of quasars at high ($z > 1.6$) redshift (Richards et al. 2011). Objects with high mass and low accretion rate are in the top left, while objects with low mass and high accretion rate are in the bottom right. RQ (RL) quasars are shown as black (red) contours/dots. RL quasars do not occupy a unique part of this parameter space (and RQ quasars still dominate the population where the RL density is highest).

Probing deeper would have wasted exposure time on objects that could already be detected and thus our proposed limit made sense for the pilot program overall. Moreover, it allowed us to identify those undetected objects where deeper exposures are unlikely to yield a detection (e.g., because they are in the Clarke Belt or are nearby a bright source, complicating the imaging and analysis). However, it is not surprising that all of our targets were not detected at the proposed depth. Thus, we propose herein to re-target objects where their star-formation rates (SFRs) are expected to be as low at 150 solar masses per year.

In Figure 2 we show the detections from our 2018B observations (in blue), upper limits (in grey) and our proposed targets (in orange). The proposed targets are indicated at the radio luminosity depth needed to detect radio from star

formation in these sources. For this estimate we have relied on an investigation of SFRs in high-redshift quasars from Harris et al. (2016) and Maddox et al. (2017). These SFRs are based on *Herschel* observations in the far-infrared (where the assumption is that the longest FIR bands are dominated by star formation and not the AGN). This FIR-based approach enables us to estimate the expected level of star formation for each object—based on predictions determined by scaling from both the optical luminosity and the measured C IV EQW. The converstion between radio luminosity and star formation rate uses the relation defined by Yun et al. (2001).

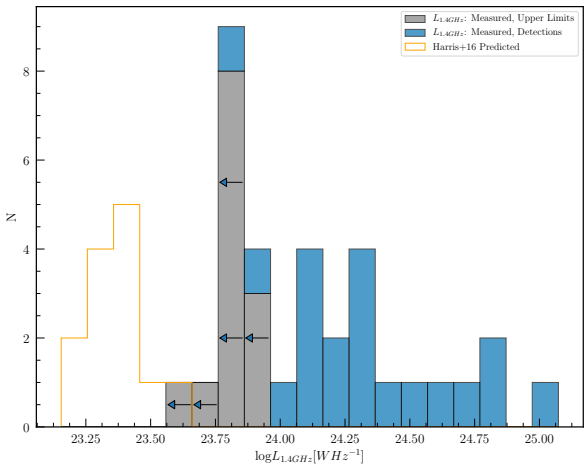

Figure 2: Comparison of measured radio luminosity (blue) to upper limits for our thirteen 2021A proposed targets (grey/arrows). Predictions based on Harris et al. (2016) for those 13 targets are shown in orange.

Based on the results shown in Figure 2 we can determine the RMS needed to achieve a 3-σ detection of that SFR. Overall, this approach suggests that we need to probe down to an average of 150 solar masses per year, which requires an S-band depth of 3.65uJy. We adopt this flux density limit for the full sample as the scatter in the predicted SFRs is $\sim$ 100 solar masses per year. Achieving this depth requires about 3 hours and is still above the confusion limit of 2.4uJy for the C-configuration using S-band.

A novel aspect of this program (not discussed further herein) is that we employ Independent Component Analysis (ICA)—a technique which identifies "like" features in the data to employ *all* of the information encoded in our ultraviolet+optical spectra. The end result is a measurement of the C IV emission-line parameters shown in in Figure 1 (EQW and "blueshift") that are robust even at the S/N of "survey depth" optical spectroscopy and can account for broad absorption line features (Rankine et al. 2020).

Targets: To identify targets for our 2018B proposal, we selected 50 representative objects that fully span the C IV parameter space shown in Figure 1, which is equivalent to fully spanning the range radiation-line-driven wind power. Crucially our targets are all *high redshift* ($z >$ 1.6) as it is only at high redshift that we encounter quasar luminosities where accretion disk winds are thought to play a truly significant role in shaping the population. The highest C IV blueshifts seen in Figure 1 are indicative of such winds. Defining a new representative sample at high redshift enables determination of whether shocks from winds are an important potential origin of radio emission in luminous quasars.

To create our sample, we started with quasars that are included in the SDSS-DR7 catalog (Schneider et al. 2007) that were selected purely on the basis of optical colors (so as not to bias towards or against their radio properties). The only other cut that we applied was to limit the sample to the 50 objects with the *lowest* redshifts in the sample (which start at $z = 1.6$ such that CIV is seen in the SDSS spectra). That selection enabled us to create a homogeneous sample that avoids evolutionary effects. As the objects fully sample the parameter space in Figure 1 we are in a good position to determine how the radio properties of quasars change as a function of the spectral diversity of quasars.

Figure 3 shows our results so far. Here we illustrate the same C IV space as in Figure 1, but only with our 50 targets and a control sample. Dark blue circles indicate detections. Red circles indicate non-detections. The size of the circle is given by the difference between the measured radio luminosity and that predicted from star formation by Harris et al. (2016). The larger sizes at high blueshift may be an indication of "excess" radio emission from wind-based shocks.

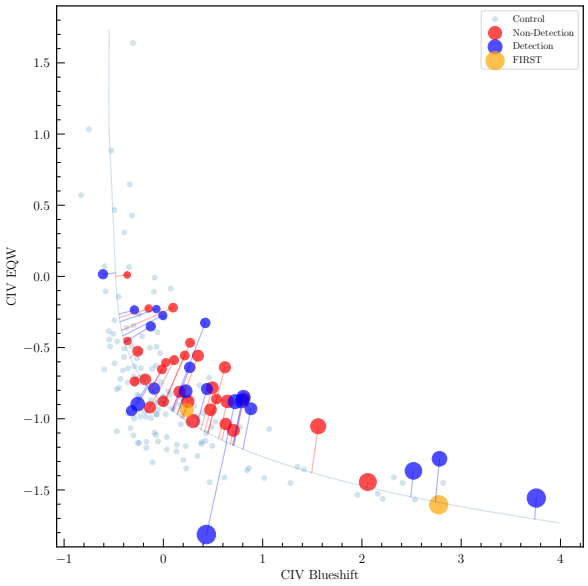

Figure 3: 2018B detections (blue) and non-detections (red) in C IV space. Point size is relative to the expected star-formation rate. Larger sizes at high blueshifts may indicate excess radio emission that could be attributed to winds.

In this followup to our pilot project, we seek to improve the limits on radio from star formation vs. winds by targetting 13 sources that were undetected at the depth achieved in 45 minutes of exposure. We exclude objects in the Clarke Belt or that have nearby bright sources, both of which limit our ability to push the limiting depth fainter than our existing observations.

Observation Details: In general, any of L-, C-, or S-band would have been appropriate to pursue this project. We preferred L or S because we recognized that existing (NVSS/FIRST) or upcoming (VLASS) survey data could be used in place of new observations. However, in C-configuration, L-band has insufficient resolution to uniquely associate any radio emission with our targets, and, as a result, we chose S-band. The current proposed observations are a continuation of the previous set of C-configuration S-band observations, and we intend to combine the uv-data from both sets of observations in order to reach the required sensitivity.

As discussed above, our current observations probe only to $\sim 300-500$ solar masses per year, while comparison with FIR results from Harris et al. (2016) suggest that we need to probe down to ~ 150 solar masses per year to achieve detections for many of our objects. To meet this goal, we aim to achieve a sensitivity of 3.65 μJy; considering the 45 minutes of on-source data in-hand, we now propose to obtain an additional 144 minutes of on-source time per target. We take into consideration the new recommended cycle time for S-band of 15 minutes, and plan on 11 calibrator cycles (13 minutes on-source + 2 minutes for slewing and phase calibration). To allow for optimal scheduling flexibility, we plan on two scheduling blocks per target, with approximately 85 minutes of target and phase calibration observations, plus 15 minutes for the initial setup and calibration. Therefore the required observing time is 200 minutes per target. As our targets span a large range of LST, this project has considerable flexibility in scheduling.

References

Barvainis et al. 1996, AJ, 111, 1431
Blundell & Beasley 1998, MNRAS, 299, 165
Blundell & Kuncic 2007, ApJL, 668, 103
Boroson, T. A. 2002, ApJ, 565, 78
Ciotti et al. 2010, ApJ, 717, 708
Condon et al. 2013, ApJ, 768, 37
Harris, K., et al. 2016, MNRAS, 457, 4179
Jarvis et al. 2019, MNRAS, 485, 2710
Kimball et al. 2011, AJ, 141, 182
Kimball et al. 2011, ApJ, 739, 29
Kimball 2020, zenodo.org/record/3942728
Kratzer & Richards 2015, AJ, 149, 61
Ivezic et al. 2002, AJ, 124, 2364
Maddox et al. 2017, MNRAS, 470, 2314
Magliochetti et al. 2016, MNRAS, 456, 431
Padovani 2017, Frontiers, 4, 35
Panessa, et al. 2019, NatureAstron., 3, 387
Rankine et al. 2020, MNRAS, 492, 4553
Richards et al. 2011, AJ, 141, 167
Schinnerer et al. 2004, AJ, 128, 1974
Schneider et al. 2010, AJ, 139, 2360
Schulze et al. 2017, ApJ, 849, 4
Sulentic et al. 2007, ApJ, 666, 757
Urry & Padovani 1995, PASP, 107, 803
Yun et al. 2001, ApJ, 554, 803
Zakamska & Greene 2014, MNRAS, 442, 784